AIP | Journal of Applied Physics

Shape memory and ferromagnetic shape memory effects in single-crystal Ni2MnGa thin films

J. W. Dong, J. Q. Xie, J. Lu, C. Adelmann, C. J. Palmstrøm et al.

Citation: J. Appl. Phys. **95**, 2593 (2004); doi: 10.1063/1.1643199
View online: http://dx.doi.org/10.1063/1.1643199
View Table of Contents: http://jap.aip.org/resource/1/JAPIAU/v95/i5
Published by the AIP Publishing LLC.

Shape memory and ferromagnetic shape memory effects in single-crystal Ni_2MnGa thin films

J. W. Dong,[a] J. Q. Xie, J. Lu,[b] C. Adelmann, and C. J. Palmstrøm[c]
Department of Chemical Engineering and Materials Science, University of Minnesota, Minneapolis, Minnesota 55455

J. Cui,[d] Q. Pan,[e] T. W. Shield, and R. D. James
Department of Aerospace Engineering and Mechanics, University of Minnesota, Minneapolis, Minnesota 55455

S. McKernan
Center for Interfacial Engineering, University of Minnesota, Minneapolis, Minnesota 55455

(Received 1 May 2003; accepted 2 December 2003)

Epitaxial Ni_2MnGa and $Ni_2Mn_{1.2}Ga_{0.8}$ thin films have been grown by molecular beam epitaxy on GaAs (001) substrates with $Sc_{0.3}Er_{0.7}As$ interlayers. Structural characterization of as-grown films confirms the epitaxially stabilized single crystal structure of the films and indicates that the films grow pseudomorphically on GaAs (001) substrates in a tetragonal structure ($a=b=5.65$ Å, $c=6.18$ Å). The films are ferromagnetic at room temperature with coercivity of ~50 Oe, saturation magnetization of ~250 emu/cm^3, and weak in-plane magnetic anisotropy. The Curie temperature of the films is found to be ~340 K. However, while the films were attached to the substrate martensitic phase transformations were not observed. In order to observe martensitic phase transformations, free-standing Ni_2MnGa bridges and cantilevers were fabricated using front and back side photolithography together with a combination of dry and wet etching. After removal of the substrate, the free-standing bridges and cantilevers showed a unique temperature dependent shape. Observation using a polarized-light optical microscope during repeated thermocycling showed large movement of the cantilevers, confirming a two-way shape memory effect in the free-standing films. Using 100 μm long free-standing bridges, field induced strain or the ferromagnetic shape memory effect was observed in a stoichiometric Ni_2MnGa sample at 135 K with the magnetic fields perpendicular to the sample surface. © *2004 American Institute of Physics.*
[DOI: 10.1063/1.1643199]

I. INTRODUCTION

Ferromagnetic shape memory alloys are a class of materials that go through a thermodynamically reversible martensitic phase transformation and demonstrate ferromagnetic behavior.[1] For bulk stoichiometric Ni_2MnGa, the Curie and martensitic phase transformation temperatures are 376 and 202 K, respectively.[2] Above 202 K, Ni_2MnGa adopts a cubic $L2_1$ crystal structure with weak magnetic anisotropy.[3] Below 202 K, it transforms into a martensitic twinned structure composed of three variants of tetragonal phase with greatly enhanced magnetic anisotropy.[3] In this low-temperature phase, external magnetic and/or stress fields can be employed to adjust the volume fraction of martensitic variants in the twinned structure by the motion of twin boundaries to minimize the total energy.[4] This rearrangement of twin variants with magnetic field results in large reversible strain, which is the mechanism for the ferromagnetic shape memory effect.[1,5] Initially, this effect was demonstrated in bulk samples of the Heusler alloy Ni_2MnGa[6] and FePd[1] by the application of moderate external magnetic fields. Recently, it has been reported to occur in Co_2NiGa,[7] Ni_2MnAl,[8] and CoNi.[9]

In order to utilize the ferromagnetic shape memory effect in devices at room temperature, the martensitic phase transformation temperature must be raised above room temperature. The phase transformation temperature of Ni_2MnGa depends critically on the composition[10–13] and it can be tuned to be above room temperature. However, modification of the composition might also change the crystal structure of martensite phase from a five layer modulated structure to a seven layer modulated, or even to a nonmodulated structure,[13] which would affect the mobility of the twin boundaries. Using Ni_2MnGa bulk single crystals, Ullakko *et al.*[6] reported reversible strain of 0.2% at 265 K. Recently, Sozinov *et al.*[14] have demonstrated strain as large as 9.5% at room temperature in orthorhombic seven layer modulated martensite of $Ni_{1.95}Mn_{1.19}Ga_{0.86}$. The ability to perform these measurements at room temperature is possible due to the dramatic change in transformation temperature according to the composition.[10–13] The large strain and the ability to tune the transformation temperature with the composition

[a]Current address: SVT Associates, Inc., Eden Prairie, MN 55344.
[b]Current address: National High Magnetic Field Laboratory, Florida State University, Tallahassee, FL 32310.
[c]Author to whom correspondence should be addressed; electronic mail: palms001@umn.edu
[d]Current address: Department of Materials and Nuclear Engineering, University of Maryland, College Park, MD 20742.
[e]Current address: Micron Technology, Inc., Boise, ID 83707.

make Ni_2MnGa a very attractive candidate for magnetic field driven actuators.[1,14,15]

Theory predicts that free-standing single crystal thin films of Ni_2MnGa could provide large work output because their deformation mode is shearing instead of bending. This would result in the work output scaling linearly with the film thickness rather than with the thickness cubed.[16] Furthermore, single crystal films allow the formation of an austenite/single variant martensite interface,[17] which is not possible in bulk materials, where only finely twinned austenite/martensite interfaces are possible.[17] The deformation mode and the ability to form austenite/single variant martensite interfaces make single crystal Ni_2MnGa films highly desirable for microelectromechanical system (MEMS) actuators.[18] Several conceptual designs for MEMS devices have been proposed by Bhattacharya *et al.*[16] based on released single crystal films with austenite/single variant martensite interfaces. Although polycrystalline films of Ni_2MnGa have been developed by several groups,[19–21] only recently have single crystal Ni_2MnGa thin films been grown.[22,23] Because the substrate imposes large constraint on the films, it is expected that only free-standing films released from the substrate will show shape memory behavior.

The theoretically proposed designs for MEMS devices require patterning and releasing of epitaxial Ni_2MnGa films from the substrates along special crystallographic directions.[16] In this article, techniques for growing, patterning and releasing 900 Å thick epitaxial stoichiometric Ni_2MnGa and $Ni_2Mn_{1.2}Ga_{0.8}$ films with expected transformation temperatures of ~200 and ~300 K, respectively, are reported. The properties of the films before and after removal of the substrate are then compared. Finally, the shape memory effect and the ferromagnetic shape memory effect within released thin film structures are studied.

II. EXPERIMENT

Ni_2MnGa films 900 Å thick were grown on (001) GaAs substrates by molecular-beam epitaxy (MBE). The growth procedure was similar to that described in Ref. 22. The GaAs substrate was overgrown with a 2500 Å thick $Al_{0.6}Ga_{0.4}As$ layer followed by 500 Å of GaAs. The $Al_{0.6}Ga_{0.4}As$ layer was added to act as an etch stop during substrate removal. To prevent reactions between the GaAs substrate and the Ni_2MnGa epilayer, a 6 monolayer thick $Sc_{0.3}Er_{0.7}As$ interlayer was deposited before Ni_2MnGa growth. *In situ* reflection high-energy electron diffraction (RHEED) was used to monitor the crystalline quality and epitaxial relationship during MBE growth.[22]

The samples were structurally characterized using x-ray diffraction (XRD), transmission electron microscopy (TEM), and Rutherford backscattering spectrometry (RBS) with channeling. At room temperature, magnetic measurements were performed using a vibrating sample magnetometer (VSM), whereas temperature dependent measurements were performed using a superconducting quantum interference device (SQUID) magnetometer.

The fabrication procedure used to make free-standing Ni_2MnGa bridges and cantilevers is schematically shown in Fig. 1. The sample substrates were first mechanically thinned and polished down to ~100 μm in thickness. Then, the 900 Å thick Ni_2MnGa film was patterned by conventional photolithography and the devices were defined using reactive ion etching. For the sample used to study the shape memory effect, the size of the bridges was 100 μm×400 μm and extended along the ⟨110⟩ direction and formed inside a 400 μm×400 μm window of GaAs that was removed. Free-standing cantilevers were also fabricated from the same film, resulting in devices of 100 μm×400 μm extending along the ⟨110⟩ direction. For the sample used in the study of the ferromagnetic shape memory effect, the free-standing bridges and cantilevers were 100 μm long and 25 μm wide.

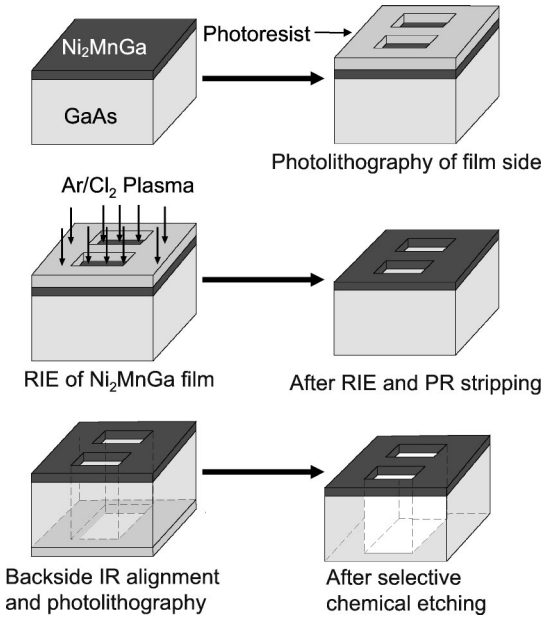

FIG. 1. Schematic illustration of the process to fabricate free-standing Ni_2MnGa bridges and cantilevers using front and back side photolithography as well as dry and selective wet chemical etching.

After front side patterning of the Ni_2MnGa film, the sample was flipped over and the GaAs substrate was lithographically patterned using a mask aligner with an infrared camera to align the pattern to the Ni_2MnGa bridges or cantilevers on the front side. The GaAs substrate in the exposed square (see Fig. 1) was then selectively etched away using a solution of H_2O_2 and NH_4OH until the etching stopped at the $Al_{0.6}Ga_{0.4}As$ layer. Subsequently, dilute HF was used to etch the 2500 Å thick $Al_{0.6}Ga_{0.4}As$ layer without removing the 500 Å thick GaAs immediately underneath the Ni_2MnGa film. Finally, this 500 Å thick GaAs was removed using a solution of H_2O_2 and NH_4OH in H_2O.

Optical observation of the shape memory effect was performed using a polarized-light microscope with a temperature stage, thus providing control of the sample temperature between −20 and 200 °C. For study of the ferromagnetic shape memory effect, the sample was mounted in a liquid helium-cooled optical cryostat equipped with a 7 T split-coil superconducting magnet and observed through an optical microscope with a large working distance.

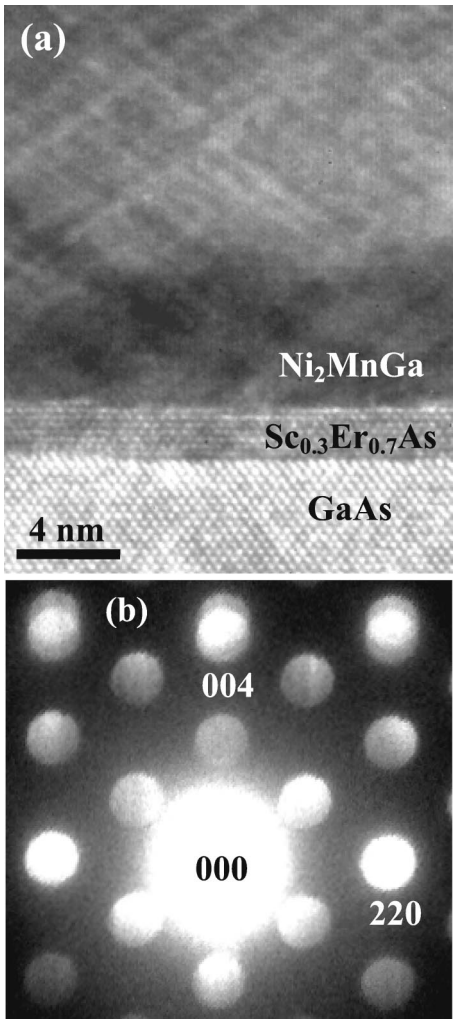

FIG. 2. (a) High-resolution cross-sectional TEM micrograph obtained for a $Ni_2MnGa/Sc_{0.3}Er_{0.7}As/GaAs$ sample. (b) Overlapping convergent beam electron diffraction patterns with the electron beam focused on both the film and the substrate. Disk splitting is clearly visible around the three $\{hh4\}$ type diffraction disks in the top row, whereas no splitting is observed for $\{hh0\}$ diffraction disks.

III. RESULTS AND DISCUSSION

A. Structural properties

Figure 2 shows a high-resolution cross-sectional TEM micrograph and a convergent beam electron diffraction (CBED) pattern of a $Ni_2MnGa/Sc_{0.3}Er_{0.7}As/GaAs$ structure. The high-resolution image in Fig. 2(a) shows that the interfaces between the GaAs substrate and the overgrown films appear to be abrupt. Moreover, no secondary phase or grain boundaries are visible in the epitaxial films. Figure 2(b) shows overlapping CBED patterns obtained from both the GaAs substrate and the Ni_2MnGa film as a result of the electron beam being focused across the interface between the film and the substrate. The two sets of diffraction disks from the substrate and the film show good registry along the in-plane direction, $\langle 110 \rangle$. However, out-of-plane disk splitting around the $\{hh4\}$ type diffractions is observed. These results indicate that the Ni_2MnGa film grows pseudomorphically on GaAs (001), resulting in a tetragonal phase with the in-plane lattice parameter of GaAs $a=b=5.65$ Å.

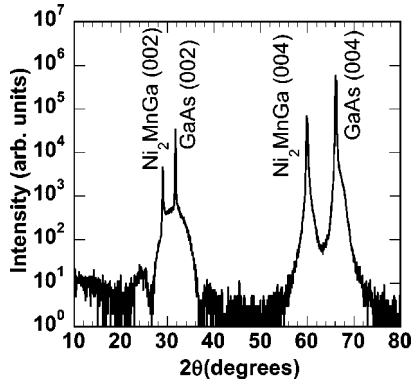

FIG. 3. X-ray θ–2θ diffraction scan of the $Ni_2MnGa/Sc_{0.3}Er_{0.7}As/GaAs$ specimen using Cu $K\alpha$ radiation.

This behavior is confirmed by the θ–2θ XRD scan of the $Ni_2MnGa/Sc_{0.3}Er_{0.7}As/GaAs$ sample shown in Fig. 3. Strong sharp (002) and (004) diffraction peaks in the Ni_2MnGa thin film are clearly evident in addition to the (002) and (004) GaAs substrate peaks. These data suggest that epitaxial relationship of $[001]_{Ni_2MnGa}//[001]_{GaAs}$. The broader weaker (002) peak and two small satellite peaks around the GaAs (002) reflection arise from the thin $Sc_{0.3}Er_{0.7}As$ interlayer.[24] No additional reflections are observed, which corroborates the absence of possible second phases, in keeping with the TEM results. Using the lattice constant of GaAs as a reference, the out-of-plane lattice constant of Ni_2MnGa was found to be 6.18 Å. Double-crystal XRD rocking curve measurements of the Ni_2MnGa (004) peak showed a full width at half maximum (FWHM) of 280 arcsec.

To further probe the crystalline quality of the epitaxial films, RBS channeling measurements were performed using 2.3 MeV He^+ ions. Figure 4 shows the RBS channeling and random spectra of a $Ni_2MnGa/Sc_{0.3}Er_{0.7}As/GaAs$ structure. After subtraction of the background, the minimum yield (χ_{min}) was obtained from the ratio of the peak areas at beam energy of ~1.55 MeV, which corresponds to the Ga peak in the epitaxial Ni_2MnGa film in the two spectra. The minimum yield of ~8% for the epitaxial $Ni_2MnGa/Sc_{0.3}Er_{0.7}As/GaAs$ structure is comparable to that in earlier studies.[25]

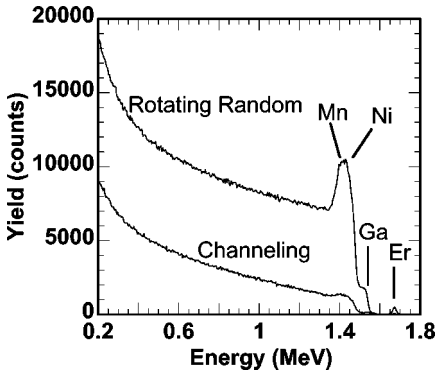

FIG. 4. RBS channeling and random spectra of the $Ni_2MnGa/Sc_{0.3}Er_{0.7}As/GaAs$ specimen using $^4He^+$ ions at beam energy of 2.3 MeV.

The formation of a pseudomorphic 900 Å thick Ni_2MnGa film on GaAs is surprising considering the fact that the lattice mismatch is 3%. This result can be explained by the high compliance of Ni_2MnGa predicted by Godlevsky and Rabe.[26] Their *ab initio* calculations showed that Ni_2MnGa has a broad free energy minimum with respect to the tetragonality of its crystal structure. Furthermore, in Fig. 2(a), two sets of fringes running along ⟨111⟩ directions with an average separation of ~1 nm can be seen. These fringes appear to be similar in form to the tweed microstructures observed in ordered compositional or strained semiconductor materials such as GaInAs.[27] It is speculated that the fringes arise from either displacement or compositional modulations within the Ni_2MnGa to accommodate the lattice mismatch between the epilayer and the GaAs substrate. The electron diffraction pattern of this epilayer also shows diffuse streaks between the positions of the lattice spots, supporting the idea of longer period, short-range modulation in the epilayer, which would also be consistent with the RBS channeling minimum yield of 8% rather than the ~3% expected for a perfect unstrained single crystal.

B. Magnetic properties

Room temperature magnetic properties of the epitaxial Ni_2MnGa films were measured by VSM. The hysteresis loops with the magnetic field applied along the three principal in-plane directions and the out-of-plane direction are shown in Fig. 5. As seen in Figs. 5(a)–5(c), no strong in-plane anisotropy is observed. The coercivity and saturation magnetization of the films were ~50 Oe and ~250 emu/cm^3, respectively. By comparing the out-of-plane [Fig. 5(d)] and in-plane hysteresis loops [Figs. 5(a)–5(c)], we see there is a hard axis parallel to the out-of plane (*c*-axis) direction even after subtraction of the demagnetization effects associated with the shape of the sample. Tickle and James[3] using bulk single crystals of Ni_2MnGa have shown that the high temperature stable cubic phase (austenite) of Ni_2MnGa is a soft magnetic material with very weak anisotropy and the martensitic tetragonal phase is relatively hard with significant magnetic anisotropy. Hence, by comparing the film and bulk magnetic properties, the soft magnetic behavior with weak in-plane anisotropy of the as-grown epitaxial films would be similar to that expected for austenitic-like phase.

Low temperature magnetic properties of the films were measured by SQUID magnetometry and the results are shown in Fig. 6. Figure 6(a) shows the hysteresis loop with the magnetic field applied along the ⟨110⟩ direction at 10 K. The coercivity and the saturation magnetization increased to ~230 Oe and ~450 emu/cm^3, respectively. Figure 6(b) shows the temperature dependence of the relative magnetization (normalized to the value at 10 K) of the epitaxial Ni_2MnGa film. The sample was first cooled down to 10 K and then warmed while constant magnetic field of 1000 Oe was applied parallel to the sample surface. The data from the cooling and warming cycles overlap with each other. From these results, the Curie temperature T_C is estimated to be ~340 K, which is close to the temperature reported for the bulk stoichiometric cubic Ni_2MnGa $L2_1$ phase (~376 K).[2]

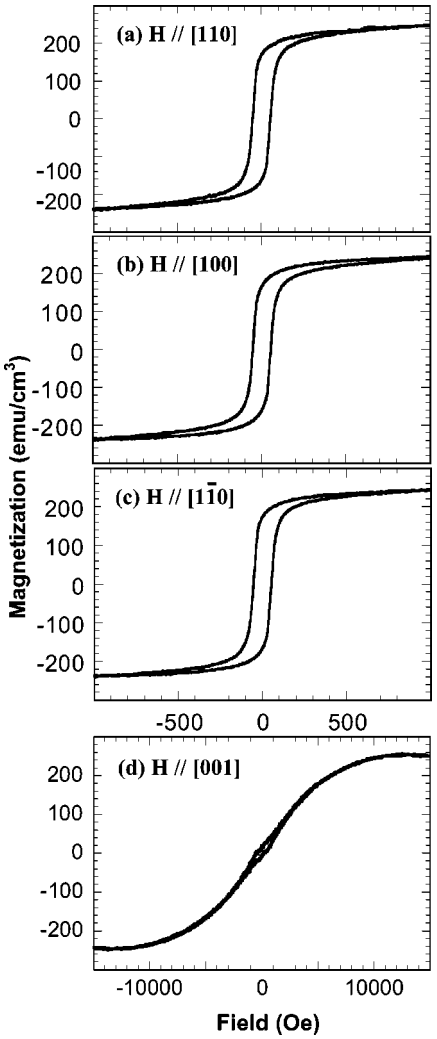

FIG. 5. Hysteresis loops measured by VSM at room temperature along (a)–(c) the three principal in-plane crystallographic directions and (d) the out-of-plane direction. The sample shows an easy plane perpendicular to the growth direction and very weak in-plane magnetic anisotropy.

The slight difference might be due to small compositional variations in the samples or to tetragonal distortion of the thin film. The magnetization versus temperature data in Fig. 6(b) show no evidence of martensitic phase transformation for the films attached to the substrate, suggesting that the presence of the substrate may inhibit phase transformation.

For actuator design, a martensitic phase transformation temperature above room temperature (RT) is desired for Ni_2MnGa. From bulk measurements,[10–13] this could be achieved by modifying the overall composition of the material, e.g., from Ni_2MnGa to $Ni_2Mn_{1.2}Ga_{0.8}$. Following this lead, a sample with a Mn-rich composition of $Ni_2Mn_{1.2}Ga_{0.8}$ was grown by MBE to realize a RT martensite structure in released films. The structural and magnetic properties of the as-grown sample were characterized by XRD and RT VSM and the results are shown in Figs. 7 and 8, respectively. From these data, it is seen that its properties are very similar to samples with stoichiometric compositions.

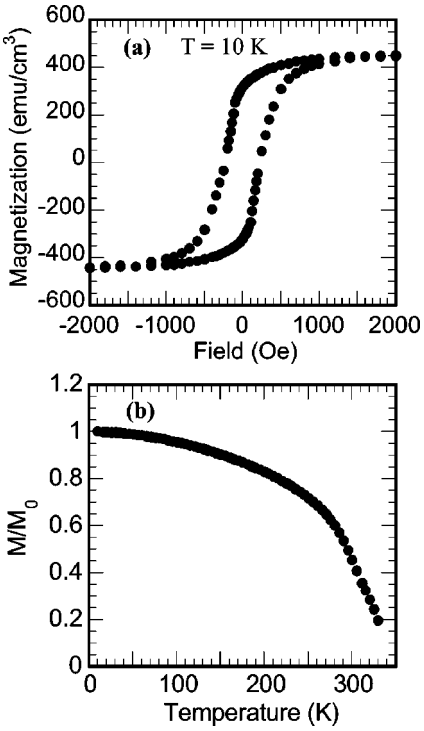

FIG. 6. Magnetic properties of an epitaxial Ni_2MnGa film obtained by SQUID measurements. (a) In-plane hysteresis loop at 10 K and (b) relative magnetization vs the temperature with a constant 1000 Oe magnetic field applied in plane.

C. Shape memory effect in free-standing $Ni_2Mn_{1.2}Ga_{0.8}$ films

Free-standing $Ni_2Mn_{1.2}Ga_{0.8}$ bridges and cantilevers were fabricated using the process shown in Fig. 1. Polarized optical micrographs and schematic illustrations of the same free-standing bridge at two different temperatures are shown in Figs. 9(a) and 9(b). The size of the bridge is 100 μm$\times$400 μm, and it extends along the $\langle 110 \rangle$ direction formed inside a 400 μm$\times$400 μm window of GaAs that was removed. The micrograph in Fig. 9(a) was taken at room temperature. It can be seen that the originally flat film pops up and forms a tent-like structure after the substrate has been removed. The roof of the tent is symmetric along its center line. The projected angle between the triangle edge and the bound end is $\sim$55°. At high temperature ($\sim$100 °C), the bridge becomes very flexible and almost reverts back to its original flat form,

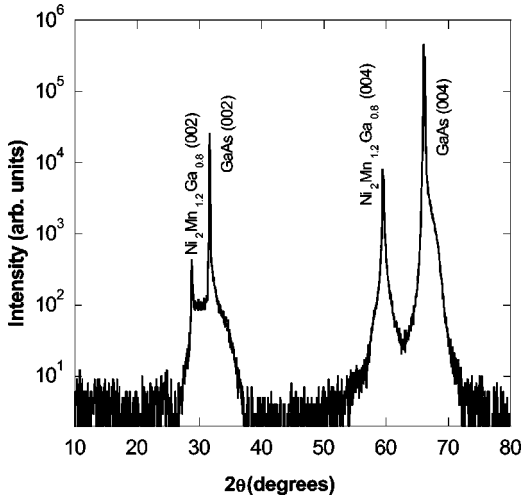

FIG. 7. θ–2θ XRD scan of an epitaxial $Ni_2Mn_{1.2}Ga_{0.8}$ film using Cu $K\alpha$ radiation.

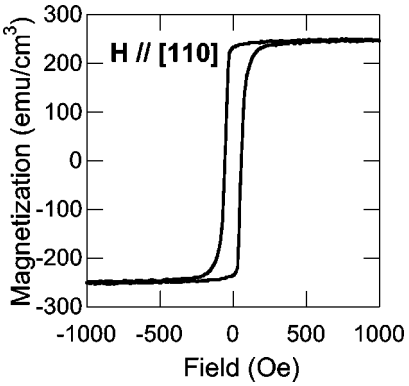

FIG. 8. In-plane magnetic hysteresis loop of the epitaxial $Ni_2Mn_{1.2}Ga_{0.8}$ film measured by VSM at RT. The coercivity of the loop is 55 Oe.

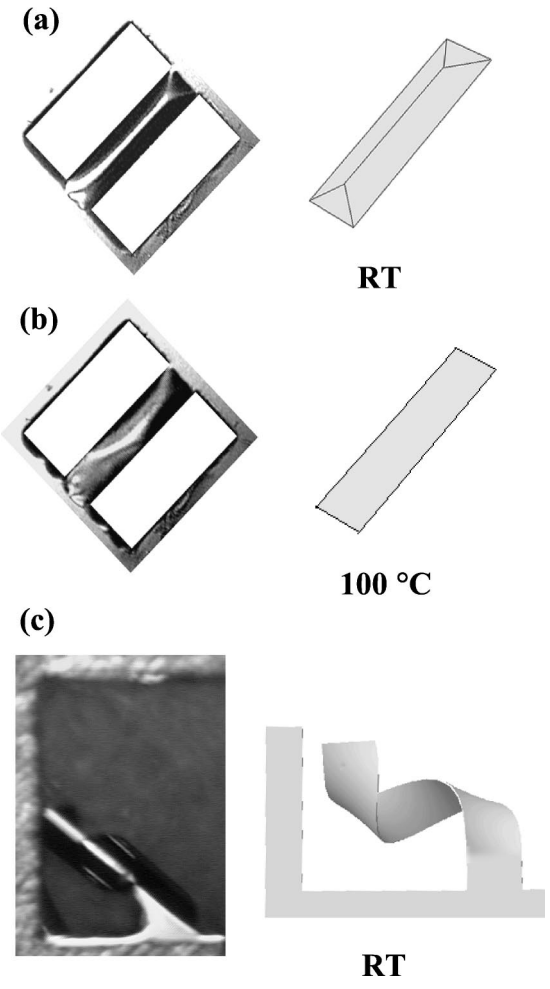

FIG. 9. Optical polarized-light microscope images and corresponding schematic illustrations showing the configurations of released $Ni_2Mn_{1.2}Ga_{0.8}$ bridges and cantilevers. (a) At room temperature, 400 μm long 100 μm wide bridges form a tent-like structure, whereas in (b) they appear flat at 100 °C. (c) Micrograph of a released cantilever at room temperature, showing a spiral-like structure.

as shown in Fig. 9(b). Furthermore, when the sample cools back down to room temperature, it transforms back into the configuration in Fig. 9(a) again.

Figure 9(c) shows a room temperature optical micrograph of a free-standing cantilever together with a schematic illustration of its shape. Instead of the tent-like structure seen for the free-standing bridges, the cantilever forms a spiral-like structure, which can be seen extending towards the upper left corner of the image. The behavior of both bridges and cantilevers suggests that the free-standing film has transformed into a martensite-like phase after removal of the substrate. This phase transformation within free-standing bridges has been confirmed by magnetic force microscopy (MFM) and SQUID measurements.[23] In addition, from those magnetic measurements, enhanced magnetic anisotropy was observed in the free-standing films.[23] Furthermore, preliminary TEM studies have shown the existence of nonmodulated martensite in the film at room temperature.[28]

Figure 10 shows a series of polarized-light optical micrographs obtained during thermocycling of a cantilever from room temperature to 160 °C and back to room temperature. Figure 10(a) was taken at room temperature and demonstrates the spiral-like configuration illustrated in Fig. 9(c). As it is heated, the cantilever film begins to straighten out its spirals [Figs. 10(b)–10(d)]. At ~150 °C, the cantilever is almost flat and is in a configuration similar to that of the unreleased film and the bridge structure at high temperature. Images taken during the cooling sequence are shown in Figs. 10(e)–10(h). The reverse phase transformation is first observed close to the free end of the cantilever as shown in Fig. 10(e). This is expected because the free end of the cantilever experiences the least amount of constraint from the GaAs substrate. In Fig. 10(e), a kink parallel to $[100]_{\text{parent phase}}$ divides the sample into transformed and untransformed parts. As the temperature is reduced further, the dark area grows mainly from the edge on the left-hand side as shown in Fig. 10(f). Then, at ~100 °C, the shape of the cantilever changes dramatically to allow initiation of the first loop [Fig. 10(g)]. Finally, at ~60 °C, the cantilever reverts back to the spiral-like structure, as shown in Fig. 10(h). This change in configuration repeated itself in all five thermocycles that were performed, which shows good repeatability of the shape memory effect. This is consistent with a two-way shape memory effect seen in bulk shape memory alloys.[29]

Typically, the temperature hysteresis of the phase transformation between $L2_1$ austenite and five layer tetragonal martensite is less than 5 °C in bulk Ni_2MnGa.[3] However, in this study, the hysteresis is larger. Tentatively, it is proposed that this is caused by both internal and external stress applied to the film. Although the film is free standing, there is still fairly large constraint from the bound end of the cantilever. This stress will make the phase transformations occur at different temperatures, which is confirmed by the fact that the fixed end of the cantilever is almost never transformed and the part close to the fixed end is always transformed later than the free end of the cantilever. Moreover, when the cantilever curves down at room temperature [Fig. 9(c)], the free end of the film touches the supporting fixture underneath it. Therefore, when phase transformation occurs, the film has to overcome frictional stress from the fixture. This process may have caused a delayed response from the film.

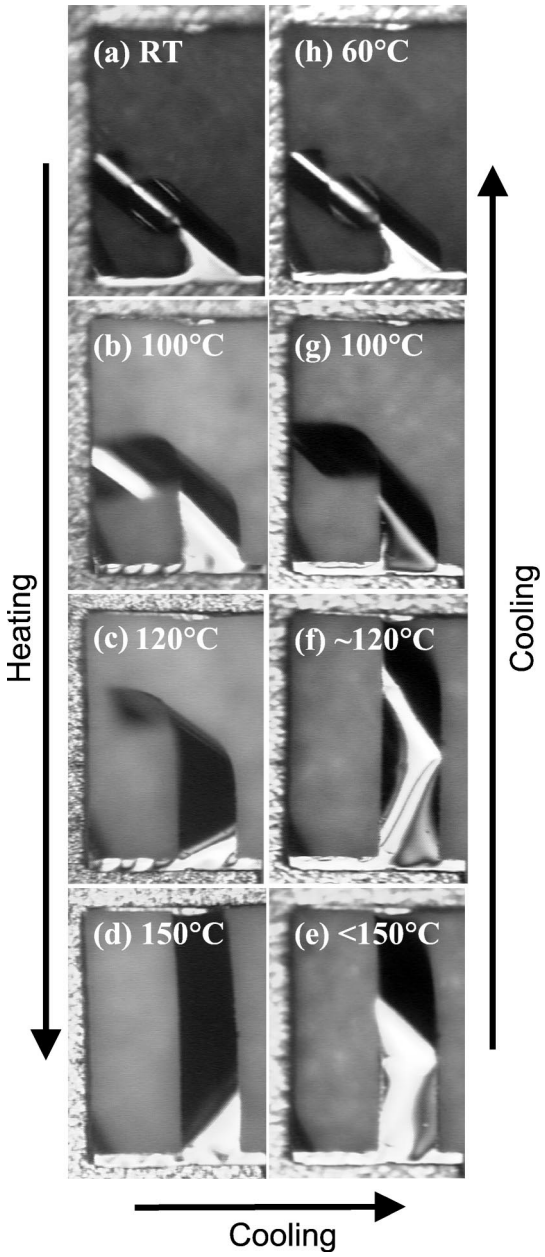

FIG. 10. Optical polarized-light microscope images of a free-standing $Ni_2Mn_{1.2}Ga_{0.8}$ cantilever at various temperatures during a thermocycle: room temperature (RT)→160 °C→RT. (a)–(d) Heating to 150 °C and (e)–(h) cooling. Uncoiling and recoiling of the spiral cantilever is clearly observed.

D. Ferromagnetic shape memory effect in free-standing Ni_2MnGa films

Experiments were first performed on the free-standing $Ni_2Mn_{1.2}Ga_{0.8}$ bridges and cantilevers to study the ferromagnetic shape memory effect at RT. However, no field-induced strain was observed in the RT martensite structure, which is believed to result from the RT martensite being a nonmodulated structure as confirmed by TEM. According to

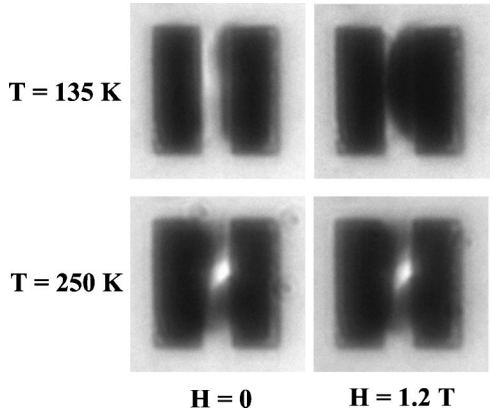

FIG. 11. Optical micrographs obtained for a 100 μm long 25 μm wide free-standing Ni_2MnGa bridge at the temperatures and magnetic fields (perpendicular to the sample surface) indicated. The long axis of the bridge is parallel to ⟨110⟩ of the as-grown film.

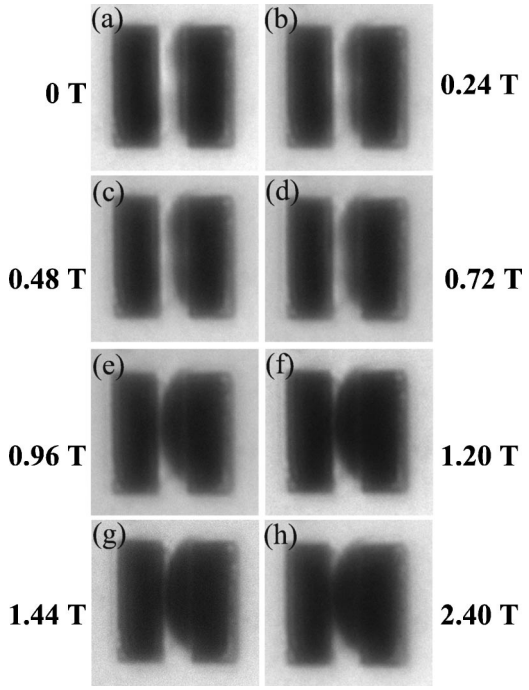

FIG. 12. Optical microscope images obtained for a 100 μm long free-standing Ni_2MnGa bridge during the application of magnetic fields perpendicular to the sample surface. The sample temperature was 135 K.

Likhachev *et al.*,[30] this type of martensite demonstrates very high twinning stress and is difficult to drive with a magnetic field.

Using a different 900 Å thick sample with composition close to that of stoichiometric Ni_2MnGa, free-standing bridges and cantilevers with 100 μm maximum length were fabricated following a process similar to that shown in Fig. 1. Figure 11 shows optical micrographs of the same bridge at temperatures of 135 and 250 K. The long axis of the bridge is parallel to the ⟨110⟩ direction of the as-grown sample. At 135 K, the bridge shows a tent-like structure similar to that in the configuration in Fig. 9(a) for a 400 μm long bridge in martensite phase at room temperature. Since the composition of this sample is nearly stoichiometric, it had to be cooled to low temperature to be transformed into martensite phase.[10–13] When the sample is heated to 250 K, a change in configuration due to the reverse thermo-martensitic phase transformation is observed. Visual observation confirmed that this phase transformation was repeatable with two distinctive transformation temperatures T_{Ms} (martensite start temperature) and T_{As} (austenite start temperature) at ~200 and ~180 K, respectively. As shown in Fig. 11, application of a magnetic field of 1.2 T perpendicular to the sample surface at 135 K caused a change in the shape of the bridge, which strongly indicates the occurrence of field induced strain or the ferromagnetic shape memory effect in the bridge. However, this latter phenomenon was not observed at 250 K, demonstrating the absence of the ferromagnetic shape memory effect in austenitic phase.

Figure 12 shows a series of optical images obtained from a free-standing bridge that was subjected to a perpendicular magnetic field at 135 K, i.e., in martensitic phase. A clear change in shape with an increase in magnetic field is observed. This change was reversible when the magnetic field was ramped down and the behavior was cyclical during the 10 magnetic field cycles performed. The precise shape of the bridge at different fields is difficult to determine because of the complex illumination conditions in the cryostat but these results clearly demonstrate the occurrence of the ferromagnetic shape memory effect in the martensitic phase of free-standing Ni_2MnGa thin films. Finally, for fields above 1.2 T, no change in shape was obvious. This might be due to the saturation of strain but clearly more quantitative measurements are required to address this issue.

IV. CONCLUSIONS

Pseudomorphic Ni_2MnGa and $Ni_2Mn_{1.2}Ga_{0.8}$ films 900 Å thick were grown by MBE on (001) GaAs substrates using a six monolayer thick $Sc_{0.3}Er_{0.7}As$ interlayer. The as-grown films have a tetragonal structure with $a=b=5.65$ Å and $c=6.18$ Å. At room temperature, the films are ferromagnetic with very weak in-plane magnetic anisotropy. The Curie temperature of the films is ~340 K. Constraint of the substrate inhibits martensitic phase transformation. Removal of the substrates to release the films enables martensitic phase transformation in the free-standing single crystal films to occur. Free-standing Ni_2MnGa bridges and cantilevers were fabricated through a combination of front and back side photolithography and etching. After removal of the GaAs substrate, $Ni_2Mn_{1.2}Ga_{0.8}$ films transform into martensitic phase at room temperature, which showed the two-way shape memory effect upon thermocycling. The ferromagnetic shape memory effect was demonstrated in free-standing stoichiometric Ni_2MnGa bridges and cantilevers at 135 K (in martensitic phase) with magnetic fields applied perpendicular to the sample surface. No ferromagnetic shape memory effect was found at higher temperatures in austenitic phase. These results support the possible use of free-standing single-crystal Ni_2MnGa film in MEMS actuators that allow remote actuation with large reversible strain.

ACKNOWLEDGMENTS

The authors would like to acknowledge the technical assistance of the Institute of Rock Magnetism at the University of Minnesota. One of the authors (J.W.D.) would also like to acknowledge doctoral dissertation fellowship support by the graduate school of the University of Minnesota. This research was supported in part by AFOSR-MURI Grant No. F49620-98-1-0433, NSF Grant No. DMS-0304326, ONR (Grant No. MURI/UMD-Z897101), and by the MRSEC program of the National Science Foundation under Award Nos. DMR-9809364 and DMR-0212302.

[1] R. D. James and M. Wuttig, Philos. Mag. A **77**, 1273 (1998).
[2] P. J. Webster, K. R. A. Ziebeck, S. L. Town, and M. S. Peak, Philos. Mag. B **49**, 295 (1984).
[3] R. Tickle and R. D. James, J. Magn. Magn. Mater. **195**, 627 (1999).
[4] R. Tickle, R. D. James, T. Shield, P. Schumacher, M. Wuttig, and V. V. Kokorin, IEEE Trans. Magn. **35**, 4301 (1999).
[5] R. C. O'Handley, J. Appl. Phys. **83**, 3263 (1998).
[6] K. Ullakko, J. K. Huang, C. Kantner, R. C. O'Handley, and V. V. Kokorin, Appl. Phys. Lett. **69**, 1966 (1996).
[7] M. Wuttig, J. Li, and C. Craciunescu, Scr. Mater. **44**, 2393 (2001).
[8] A. Fujita, K. Fukamichi, F. Gejima, and K. Ishida, Appl. Phys. Lett. **77**, 3054 (2000).
[9] Y. Liu *et al.*, Appl. Phys. Lett. **78**, 3660 (2001).
[10] A. N. Vasil'ev *et al.*, Phys. Rev. B **59**, 1113 (1999).
[11] K. Ullakko, Y. Ezer, A. Sozinov, G. Kimmel, P. Yakovenko, and V. K. Lindroos, Scr. Mater. **44**, 475 (2001).
[12] V. A. Chernenko, E. Cesari, V. V. Kokorin, and I. N. Vitenko, Scr. Metall. Mater. **33**, 1239 (1995).
[13] J. Pons, V. A. Chernenko, R. Santamarta, and E. Cesari, Acta Mater. **48**, 3027 (2000).
[14] A. Sozinov, A. A. Likhachev, N. Lanska, and K. Ullakko, Appl. Phys. Lett. **80**, 1746 (2002).
[15] S. J. Murray, M. A. Marioni, A. M. Kukla, J. Robinson, R. C. O'Handley, and S. M. Allen, J. Appl. Phys. **87**, 5774 (2000).
[16] K. Bhattacharya, A. DeSimone, K. F. Hane, R. D. James, and C. J. Palmstrøm, Mater. Sci. Eng., A **273–275**, 685 (1999).
[17] M. S. Wechsler, D. S. Lieberman, and T. A. Reed, TMS JOM **197**, 1503 (1953).
[18] K. Bhattacharya and R. D. James, J. Mech. Phys. Solids **47**, 531 (1999).
[19] M. Suzuki, M. Ohtsuka, T. Suzuki, M. Matsumoto, and H. Miki, Mater. Trans., JIM **40**, 1174 (1999).
[20] J. Ahn, N. Cheng, T. Lograsso, and K. M. Krishnan, IEEE Trans. Magn. **37**, 2141 (2001).
[21] M. Wuttig, C. Craciunescu, and J. Li, Mater. Trans., JIM **41**, 933 (2000).
[22] J. W. Dong, L. C. Chen, C. J. Palmstrøm, R. D. James, and S. McKernan, Appl. Phys. Lett. **75**, 1443 (1999).
[23] Q. Pan, J. W. Dong, J. Cui, C. J. Palmstrøm, and R. D. James, J. Appl. Phys. **91**, 7812 (2002).
[24] L. C. Chen, J. W. Dong, B. D. Schultz, C. J. Palmstrøm, J. Berezovsky, A. Isakovic, P. A. Crowell, and N. Tabat, J. Vac. Sci. Technol. B **18**, 2057 (2000).
[25] J. W. Dong, J. Lu, J. Q. Xie, L. C. Chen, R. D. James, S. McKernan, and C. J. Palmstrøm, Physica E **10**, 428 (2001).
[26] V. V. Godlevsky and K. M. Rabe, Phys. Rev. B **63**, 134407/1 (2001).
[27] D. M. Follstaedt, J. L. Reno, E. D. Jones, S. R. Lee, A. G. Norman, H. R. Moutinho, A. Mascarenhas, and R. D. Twesten, Appl. Phys. Lett. **77**, 669 (2000).
[28] J. W. Dong, S. McKernan, J. Q. Xie, D. W. Sievers, C. J. Palmstrøm, and R. D. James (unpublished).
[29] K. Otsuka and C. M. Wayman, *Shape Memory Materials* (Cambridge University Press, New York, 1999).
[30] A. A. Likhachev, A. Sozinov, and K. Ullakko, Proc. SPIE **4333**, 197 (2001).